Cell Tissue Res (2012) 347:803–813
DOI 10.1007/s00441-011-1308-1

REGULAR ARTICLE

Fabrication and evaluation of biomimetic-synthetic nanofibrous composites for soft tissue regeneration

Albert O. Gee · Brendon M. Baker · Amy M. Silverstein · Giana Montero · John L. Esterhai · Robert L. Mauck

Received: 13 June 2011 / Accepted: 15 December 2011 / Published online: 28 January 2012

Abstract Electrospun scaffolds hold promise for the regeneration of dense connective tissues, given their nanoscale topographies, provision of directional cues for infiltrating cells and versatile composition. Synthetic slow-degrading scaffolds provide long-term mechanical support and nanoscale instructional cues; however, these scaffolds suffer from a poor infiltration rate. Alternatively, nanofibrous constructs formed from natural biomimetic materials (such as collagen) rapidly infiltrate but provide little mechanical support. To take advantage of the positive features of these constructs, we have developed a composite scaffold consisting in both a biomimetic fiber fraction (i.e., Type I collagen nanofibers) together with a traditional synthetic (i.e., poly-[ε-caprolactone], PCL) fiber fraction. We hypothesize that inclusion of biomimetic elements will improve initial cell adhesion and eventual scaffold infiltration, whereas the synthetic elements will provide controlled and long-term mechanical support. We have developed a method of forming and crosslinking collagen nanofibers by using the natural crosslinking agent genipin (GP). Further, we have formed composites from collagen and PCL and evaluated the long-term performance of these scaffolds when seeded with mesenchymal stem cells. Our results demonstrate that GP crosslinking is cytocompatible and generates stable nanofibrous type I collagen constructs. Composites with varying fractions of the biomimetic and synthetic fiber families are formed and retain their collagen fiber fractions during in vitro culture. However, at the maximum collagen fiber fractions (20%), cell ingress is limited compared with pure PCL scaffolds. These results provide a new foundation for the development and optimization of biomimetic/synthetic nanofibrous composites for in vivo tissue engineering.

Keywords Tissue engineering · Mechanical properties · Nanofiber · Scaffolds · Electrospinning · Mesenchymal stem cells

This work was supported by the National Institutes of Health (R01 AR056624, RLM), The Department of Veterans' Affairs (I01 RX000174, JLE) and the Penn Center for Musculoskeletal Disorders (P30 AR050950, RLM). Additional support was provided by the Penn Department of Orthopaedic Surgery (AOG) and a graduate fellowship from the National Science Foundation (BMB).

A. O. Gee · B. M. Baker · A. M. Silverstein · G. Montero · J. L. Esterhai · R. L. Mauck
McKay Orthopaedic Research Laboratory,
Department of Orthopaedic Surgery, University of Pennsylvania,
Philadelphia, PA 19104, USA

B. M. Baker · A. M. Silverstein · G. Montero · R. L. Mauck
Department of Bioengineering, University of Pennsylvania,
Philadelphia, PA 19104, USA

J. L. Esterhai · R. L. Mauck
Philadelphia VA Medical Center,
Philadelphia, PA 19104, USA

R. L. Mauck (✉)
Orthopaedic Surgery and Bioengineering, McKay Orthopaedic Research Laboratory, Department of Orthopaedic Surgery,
University of Pennsylvania,
424G Stemmler Hall, 36th Street and Hamilton Walk,
Philadelphia, PA 19104, USA
e-mail: lemauck@mail.med.upenn.edu
URL: http://www.med.upenn.edu/orl/people/mauck/mauck.shtml

Introduction

Collagen is the principal constituent of the extracellular matrix (ECM) of most dense connective tissues and, as such, defines the microenvironmental milieu in which cells reside. In fiber-reinforced musculoskeletal tissues, collagen fibers are highly organized and generate the direction-dependent mechanical properties critical to the function of

these structures (Mauck et al. 2009). Given its primary role in native tissues, collagen is particularly attractive as a biomaterial for tissue engineering applications in which scaffolds are coupled with cells to repair or regenerate damaged tissues (Yannas et al. 2010). One method for producing collagen-based scaffolds is through electrospinning (Barnes et al. 2007a; Matthews et al. 2002; Shields et al. 2004; Zhong et al. 2006; Venugopal et al. 2005; Li et al. 2005a; Buttafoco et al. 2006; Rho et al. 2006; Sefcik et al. 2008). This technique yields nanoscale to micronscale fibers similar in diameter to those of the native ECM (Barnes et al. 2007a; Li et al. 2005b; Baker et al. 2009a; Pham et al. 2006a). For the engineering of orthopaedic tissues, methods have been devised to electrospin fibers into aligned arrays that can recapitulate the anisotropy of fiber-reinforced tissues (Li et al. 2007; Nerurkar et al. 2007; Courtney et al. 2006; Ayres et al. 2006). We have shown that nanofibrous scaffolds containing a single slow-degrading synthetic fiber population can promote the formation of organized and mechanically robust tissue-engineered constructs with application to the knee meniscus (Baker et al. 2009b) and the annulus fibrosus of the intervertebral disc (Nerurkar et al. 2009). Although a number of polymers have been electrospun in this aligned format, collagen-based scaffolds are especially promising as they provide a biomimetic interface for cell attachment (Matthews et al. 2002; Teo and Ramakrishna 2006). Indeed, early reports from Telemeco and coworkers (2005), using randomly organized nanofibrous constructs, demonstrate that collagen-based (but not synthetic) scaffolds can be infiltrated completely when placed in vivo.

Whereas electrospun collagen scaffolds are of great interest to the tissue engineering community, one major drawback is their inherent instability in aqueous environments. To address this, various crosslinking agents including glutaraldehyde (GA), 1-ethyl-3-(3-dimethylaminopropyl) carbodiimide hydrochloride and N-hydroxysuccinimide chemistries have been used to stabilize the fibers (Shields et al. 2004; Zhong et al. 2006; Barnes et al. 2007b). However, these chemicals often prove cytotoxic or excessively laborious in application and do not necessarily preserve the nanoscale topography of the fibers (Shields et al. 2004). Moreover, even with crosslinking, the mechanical properties of collagen-based nanofibrous scaffolds decrease dramatically with rehydration (Barnes et al. 2007b). Thus, pure collagen nanofibrous scaffolds cannot function in a context in which load-bearing is necessary immediately upon implantation.

In this study, we have assessed genipin (GP) as an alternative crosslinker for preserving the structure and mechanical characteristics of type I collagen nanofibrous scaffolds. GP, a natural extract from the Gardenia flower, has been employed in crosslinking porcine pericardium and gelatin microspheres and is considered to be less cytotoxic than most other agents (Sung et al. 2000,2001; Liang et al. 2003). In this work, we have compared the crosslinking of collagen nanofibers by GP with that by glutaraldehyde (GA) vapor, the standard method in the literature. Previous comparisons between these agents using gelatin microspheres have demonstrated that GA treatment results in less stability than GP treatment. We hypothesize that GP will preserve the biomimetic properties of collagen nanofibers, demonstrating improved cell adhesion over synthetic poly-(ε-caprolactone) (PCL) nanofibers. Additionally, we postulate that GP will stabilize collagen nanofibers in aqueous solution and maintain scaffold mechanical properties at levels comparable with those of other crosslinking methods.

Because of the decrease in mechanical properties that occurs with hydration of collagen (and other biologic/protein-based) nanofibrous scaffolds, a number of methodologies have been developed to take advantage of the beneficial aspects of collagen, while improving overall scaffold mechanics. Most popular is the inclusion of collagen (or another biologic moiety) in the same spinning solution as a synthetic polymer (Stankus et al. 2008, Ekaputra et al. 2008, 2011). For this, solvents must be used that are compatible with both the biologic molecule in question and with the synthetic carrier polymer. For example, Stitzel and co-workers have spun collagen, elastin and poly-(lactide-co-glycolide) from the same solution and shown that individual fibers containing natural and synthetic elements are more cell-adhesive than pure synthetic fibers and that scaffolds formed in this way retain their mechanical properties upon hydration (Stitzel et al. 2006; Lee et al. 2007). Similar approaches have been taken with a number of other biologic materials that show the same aqueous instability in nanofibrous format as collagen (Sell et al. 2006). In addition to co-spinning the biologic and synthetic elements together into one fiber, others have coupled the biologic moiety to the previously formed synthetic fiber (Ma et al. 2005; Casper et al. 2005, 2007). For example, gelatin fragments have been grafted onto PCL fibers, showing enhanced biologic activity of the modified scaffold (Ma et al. 2005). Several potential drawbacks exist to these methods, however. In the case of co-spinning mixed solutions of collagen (or other biologic molecules) and synthetics, the distribution of components in the resulting fibers is difficult to assess and control. The amount of the biomolecule that will be present at the surface of synthetic fibers, or whether natural cell-mediated degradation mechanisms can act upon those molecules trapped within the fibers, is unclear. In the case of surface-coupled molecules, the synthetic backbone will persist, even after cellular interaction and/or degradation of this surface-bound molecule. This is particularly important given the slow infiltration observed in purely synthetic nanofiber networks (Baker et al. 2009b; Telemeco et al. 2005; Pham et

al. 2006b). If cells cannot degrade the fibers, then cell attachment but not cell infiltration, will be improved.

To address this issue, we have developed a system for making composites with multiple (but distinct) fiber families by using a multi-jet electrospinning approach (Baker et al. 2009c). Multi-jet spinning has previously been described for combining a variety of synthetic fibers, in which each fiber fraction imparts different mechanical attributes to the composite structure (Ding et al. 2004; Kidoaki et al. 2005; Stella et al. 2008; Baker et al. 2008; Ionescu et al. 2010; Ladd et al. 2011). For instance, in a recent report, we have shown that the inclusion of increasing amounts of "sacrificial" poly-(ethylene oxide) (PEO) nanofibers can expedite cellular colonization by increasing the scaffold porosity from the outset (Baker et al. 2008). One limitation of our study was the immediate dissolution of the sacrificial fiber fraction in which pores were created immediately throughout the scaffold, far in advance of cell migration. In an alternative approach, Ekaputra and colleagues have developed a combined electrospinning/electrospraying technique wherein PCL fibers including collagen are spun at the same time that biologic hyaluronic-acid-based materials are electrosprayed; these composites with biologic inclusions are more rapidly infiltrated than fiber-alone scaffolds (Ekaputra et al. 2008, 2011). In the current study, we hypothesized that the judicious combinations of type I collagen and PCL nanofibers into a composite scaffold will enhance cellularity and infiltration, with the PCL fraction maintaining the mechanical properties of the scaffold over long culture durations. We also hypothesized that collagen fiber fractions will enhance the bioactivity of scaffolds and yet be subject to remodeling and breakdown via cell-mediated processes as they infiltrate the scaffold. To examine this phenomenon, two distinct fiber populations (PCL and collagen) have been electrospun into the same scaffold, at two different levels of biomimetic inclusion: low (10% collagen) and high (20% collagen) levels. The mechanical properties, biochemical content and mesenchymal stem cell (MSC) infiltration of the constructs have been evaluated with time in culture in a chemically defined in vitro culture environment.

Materials and methods

Electrospinning of collagen nanofibers

Type I collagen nanofibers were formed based on a protocol modified from Bowlin and colleagues (Matthews et al. 2002). Collagen type I from calf skin (Sigma, St. Louis, Mo., USA) was dissolved in 1,1,1,3,3,3-hexafluoro-2-propanol (HFIP) at a concentration of 80 mg/ml. After centrifugation at 1000*g* for 20 min, a homogenous collagen solution was obtained. This solution was expressed through a 20-gauge blunt-ended needle (spinneret) along a 15-kV electric field over a 12.5-cm air gap. For initial characterization and cell interaction studies, thin layers of collagen fibers were collected onto glass microscope slides. For mechanical testing, thicker mats were collected on either a grounded plate or a mandrel rotating at ~10 m/s to obtain non-aligned or aligned scaffolds, respectively (Li et al. 2007; Baker and Mauck 2007). For comparison, PCL (Sigma-Aldrich, St. Louis, Mo., USA) was prepared in a tetrahydrofuran/dimethylformamide solution as previously described (Li et al. 2007; Baker and Mauck 2007) and expressed through an 18-G blunt-ended spinneret charged to 13 kV over a 20-cm air gap. All fibers and scaffolds were exposed to germicidal UV light in a biosafety cabinet for 1 h prior to use in cell seeding studies.

Crosslinking of collagen nanofibers

Because collagen nanofibers are inherently unstable in an aqueous environment, crosslinking methodologies were used to stabilize nanofibrous films and scaffolds. Collagen nanofiber films and scaffolds were crosslinked with either GP or GA. For GP crosslinking, fibers on slides or whole fiber mats were submerged in 0.4 M GP dissolved in 100% ethanol for 48 h at 37°C (Sung et al. 2000, 2001; Liang et al. 2003). GA crosslinking was achieved by incubation of samples in a vapor chamber containing a 1:1 solution of GA:H_2O for 24 h at 25°C (Zhong et al. 2006). After GA fixation, scaffolds were washed with 100% ethanol and submerged in 0.1 M glycine to quench residual aldehydes. To visualize scaffolds and films before and after crosslinking, samples were lyophilized, sputter-coated with Au/Pd and viewed by scanning electron microscopy (SEM). Collagen fibers pre- and post-crosslinking were examined in a dry state.

Cell culture and assessment of morphology

After the crosslinking step, thin layers of collagen nanofibers on glass slides were rinsed once in 100% ethanol and three times in phosphate-buffered saline (PBS) prior to cell seeding. Slides were seeded with ovine mesenchymal stem cells (MSCs) that were expanded through passage 2 (Huang et al. 2009). In duplicate fashion, 1 ml of media containing 5×10^4 cells were pipetted onto each slide, followed by incubation under 5% CO_2 at 37°C for 4, 8, 12, or 24 h to allow cell adhesion. At each time point, cells were fixed in 4% paraformaldehyde and stained with phalloidin/Alexa Fluor 488 and 4,6-diamidino-2-phenylindole (DAPI) to visualize the actin cytoskeleton and nucleus, respectively (Nathan et al. 2009). Images were acquired at 20× magnification by using a Nikon T30 inverted fluorescent microscope.

Mechanical evaluation of nanofibrous collagen scaffolds

Uniaxial tensile testing was performed on dry as-spun samples (~15×3.5 mm) cut either parallel (fiber) or perpendicular (trans) to the prevailing fiber direction (Li et al. 2007; Baker and Mauck 2007). Additional crosslinked samples were tested after submersion in PBS. Thickness was determined by using an LVDT system and width was measured with digital calipers. Samples were extended to failure at a constant strain rate of 0.1%/s. The tensile modulus was calculated from the linear region of the stress-strain curve.

Composite scaffold formation and analysis

Composite scaffolds were formed from individual fibers of collagen and PCL. PCL and type I collagen spinning solutions were prepared as described above. A sheet of ~0.5 mm in thickness containing distinct PCL and collagen fibers was electrospun via three separate spinnerets (one containing PCL solution, two containing collagen solution), focused on a common rotating mandrel to instill fiber-alignment by using a custom-made device (Baker et al. 2009c). Control scaffolds containing PCL alone were electrospun by using a single jet. Test samples from the composite scaffold were submerged in 90% ethanol followed by distilled H_2O to remove collagen from the composite. After desiccation and weighing, the percentage of the collagen in the original mat was determined by fractional mass loss. Scaffolds (5×30 mm, long axis in fiber direction) of 10% (Low) and 20% (High) collagen by mass were prepared for cell seeding. Pure PCL scaffolds were likewise prepared as controls. All scaffolds were crosslinked in 0.8 M GP in 100% ethanol for 5 days at 37°C and stored in 100% ethanol until seeding. Acellular strips were cross-sectioned and stained with Picrosirius Red (PSR) before and after crosslinking and hydration to verify the retention of collagen with GP treatment.

Long-term in vitro culture of PCL-collagen composite scaffolds

For long-term cell seeding studies, scaffolds (PCL, GP-stabilized "Low" collagen content and GP-stabilized "High" collagen content) were hydrated and sterilized through a graded series of ethanol/double-distilled H_2O, terminating in 100% PBS. Bovine MSCs were seeded at a density of 1 million cells per scaffold and cultured for 9 weeks in a chemically defined medium (high glucose DMEM with 1× antibiotics/antimycotics, 0.1 μM dexamethasone, 50 μg/ml ascorbate 2-phosphate, 40 μg/ml L-proline, 100 μg/ml sodium pyruvate, 6.25 μg/ml insulin, 6.25 μg/ml transferrin, 6.25 ng/ml selenous acid, 1.25 mg/ml bovine serum albumin and 5.35 μg/ml linoleic acid; Baker et al. 2009b) containing 10 ng/ml transforming growth factor-β3 (R&D Systems, Minneapolis, Minn., USA). On days 21, 42 and 63, constructs were mechanically tested under tension as above. After mechanical testing, all samples were papain-digested (Mauck et al. 2006) and the content of DNA, sulfated glycosaminoglycan (s-GAG) and collagen was determined by using the Picogreen double-stranded DNA (dsDNA) kit (Molecular Probes, Eugene, Ore., USA), DMMB dye-binding (Farndale et al. 1986) and hydroxyproline assay (Stegemann and Stalder 1967), respectively. Cross sections of the constructs were stained with PSR and DAPI to visualize collagen content and location of cell nuclei, respectively. Nuclear position with respect to the boundary was quantified from DAPI-stained cross sections for each sample. Briefly, a custom MATLAB script (Baker et al. 2008) was used to identify the position of each nucleus in the image with respect to the scaffold boundary. Position was binned into one of four equal regions, with 0% indicating a cell at the scaffold edge and 100% indicating a cell that had infiltrated to the center of the scaffold (see below). Data are presented as means ± SD of five to six samples per group per time point. Statistical significance was determined by analysis of variance with Bonferroni post-hoc tests.

Results

Formation and crosslinking of type I collagen nanofibrous scaffolds

Using established protocols, type I collagen nanofibers were successfully electrospun into non-aligned and aligned meshes (Fig. 1a, b). Samples that were not crosslinked dissolved upon submersion in PBS, whereas GP- and GA-crosslinked scaffolds endured extensive washing. Inspection of fiber morphology by SEM showed that, whereas GA-treated fibers swelled and fused to give a slab-like appearance, GP crosslinking preserved the integrity of the collagen nanofibers (Fig. 1c–e). MSCs seeded onto collagen nanofibers (both GA- and GP-crosslinked) showed rapid adhesion and elongation of cell processes along individual fibers, even at the earliest time point of 4 h (not shown). Conversely, MSCs seeded on PCL showed poor attachment and little tracking along fibers at 4 h. By 24 h, MSCs on PCL scaffolds had adhered with small processes being evident, whereas MSCs on both GA- and GP-crosslinked scaffolds were well-spread at this time point (Fig. 2). Tensile testing of aligned collagen scaffolds revealed the effect of fiber organization on mechanical anisotropy: samples extended in the fiber direction had moduli approximately eight times higher (~80 MPa) than those extended in the transverse direction (Fig. 3a, $P<0.005$). However, after crosslinking and hydration, markedly lower moduli were observed in both GA- and GP-treated scaffolds (lowering the modulus in the fiber direction to ~0.5-1 MPa),

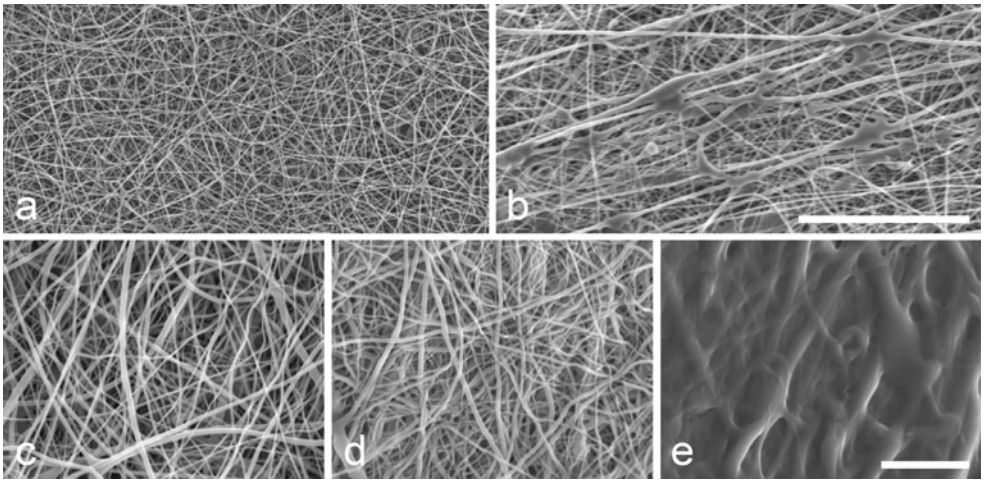

Fig. 1 Morphology of electrospun collagen nanofibers upon crosslinking and hydration. Scanning electron micrographs (SEM) of (**a**) non-aligned, (**b**) aligned, (**c**) pre-crosslinked, (**d**) GP-crosslinked post-submersion and (**e**) GA-crosslinked post-submersion. *Bars* 50 μm (*top*), 10 μm (*bottom*)

with no difference being found between these two groups (Fig. 3b, $P>0.14$).

Formation and analysis of PCL-collagen composites

To address the poor mechanics of crosslinked hydrated nanofibrous scaffolds formed from pure collagen, composites were formed with fiber families including both a stiff slow-degrading PCL fiber fraction and a biomimetic type I collagen fiber fraction. For this, two jets containing collagen solution and one jet containing PCL were spun and collected simultaneously on a common rotating mandrel. Contrary to expectations based on delivery volumes, in which nearly 2/3 of the scaffold should have been composed of collagen, the highest mass loss noted upon submersion in ethanol or water was the order of 20%. This finding was probably attributable to PCL collecting in a much more focused manner than the disperse collection of collagen fibers. To visualize the presence of collagen before and after crosslinking, acellular composite scaffolds with a range of collagen fiber fractions (either Low [10%] or High [20%] collagen) were stained with PSR. Whereas little background staining was observed in PCL controls, rich staining was seen in the collagen-containing composite scaffolds. Importantly, washes in PBS removed this collagen fiber fraction in non-crosslinked samples but did not alter staining intensity in GP-crosslinked samples (Fig. 4).

To examine the cellular interaction and maturation of these composite scaffolds, both Low and High collagen content scaffolds were crosslinked with GP, seeded with MSCs and cultured in a chemically defined in vitro environment for up to 9 weeks. Mechanical assessment showed that the presence of collagen in the composite decreased the overall modulus on day 21, with Low and High composite constructs having a significantly lower modulus than PCL-alone constructs ($P<0.05$, Fig. 5a). As expected, increasing collagen content was found in Low and High composites on day 21 compared with PCL controls ($P<0.05$, Fig. 5c), indicative of the inclusion and retention of the initial collagen fiber families. With longer periods of culture, all seeded constructs increased in mechanical properties by day 63

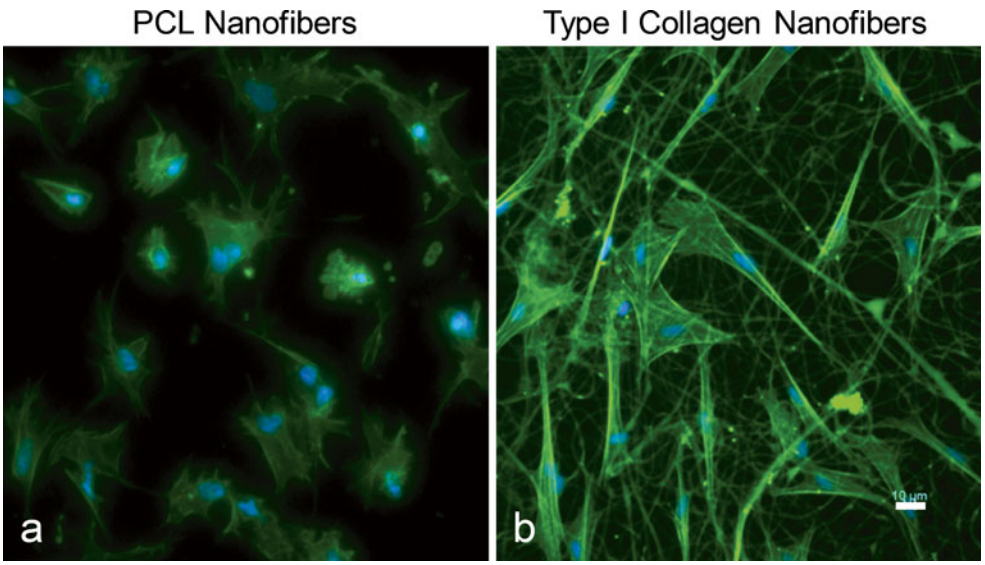

Fig. 2 Cell adhesion to and morphology on synthetic (PCL) and biomimetic (collagen) nanofibers. Phalloidin staining of actin (*green*) and DAPI staining of cell nuclei (*blue*) at 24 h post-seeding on PCL (**a**) and collagen (**b**) nanofiber films. Note that collagen nanofibers autofluoresce (*green, right*). *Bar* 10 μm

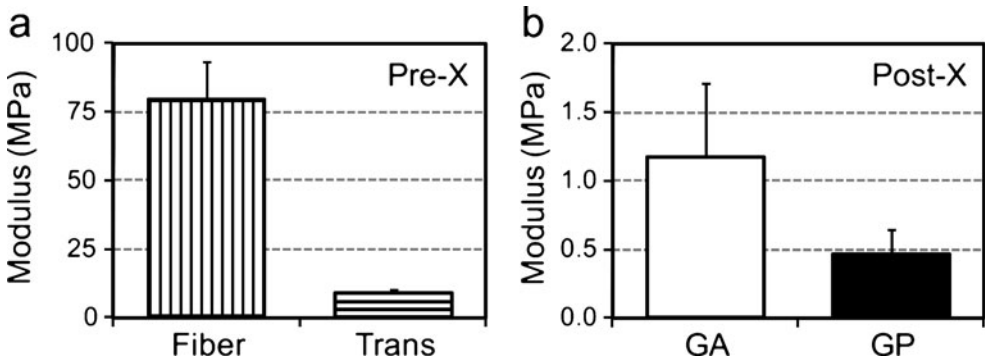

Fig. 3 Mechanics of type I collagen nanofibrous scaffolds before and after crosslinking. **a** Tensile modulus of dry pre-crosslinked (*pre-X*) collagen scaffolds in the fiber and transverse to the fiber directions. **b** Tensile modulus in the fiber direction of GA- and GP-crosslinked (*post-X*) collagen scaffolds hydrated in phosphate-buffered saline; $n=4$ per group

(Fig. 5a). Interestingly, PCL constructs increased in DNA, collagen and GAG content with time, whereas Low collagen composite constructs showed only increasing DNA, with GAG and collagen contents remaining unchanged. Composites containing High collagen fiber fractions at the outset increased in DNA content, showed no change in GAG content and slightly decreased in collagen content with time (Fig. 5b–d), presumably a result of the electrospun collagen slowly leaching from the composite system. Comparisons between groups at day 63 showed that PCL scaffolds had a higher DNA and GAG content ($P<0.05$) than composite constructs. Moreover, by day 63, DAPI-stained cross-sections showed that PCL constructs achieved the greatest degree of cell infiltration and matrix deposition, followed by the Low composite constructs (Fig. 6). Composites with the highest collagen fiber fraction showed the poorest cell infiltration. Quantification of the position of each cell with respect to the scaffold periphery further underscored these histological findings (Fig. 7). Namely, on day 63, ~60% of all cells were located in the outer 25% of the scaffold for both the High and Low collagen composites, whereas a significantly lower fraction (36%, $P<0.01$ vs. High and Low groups) of the

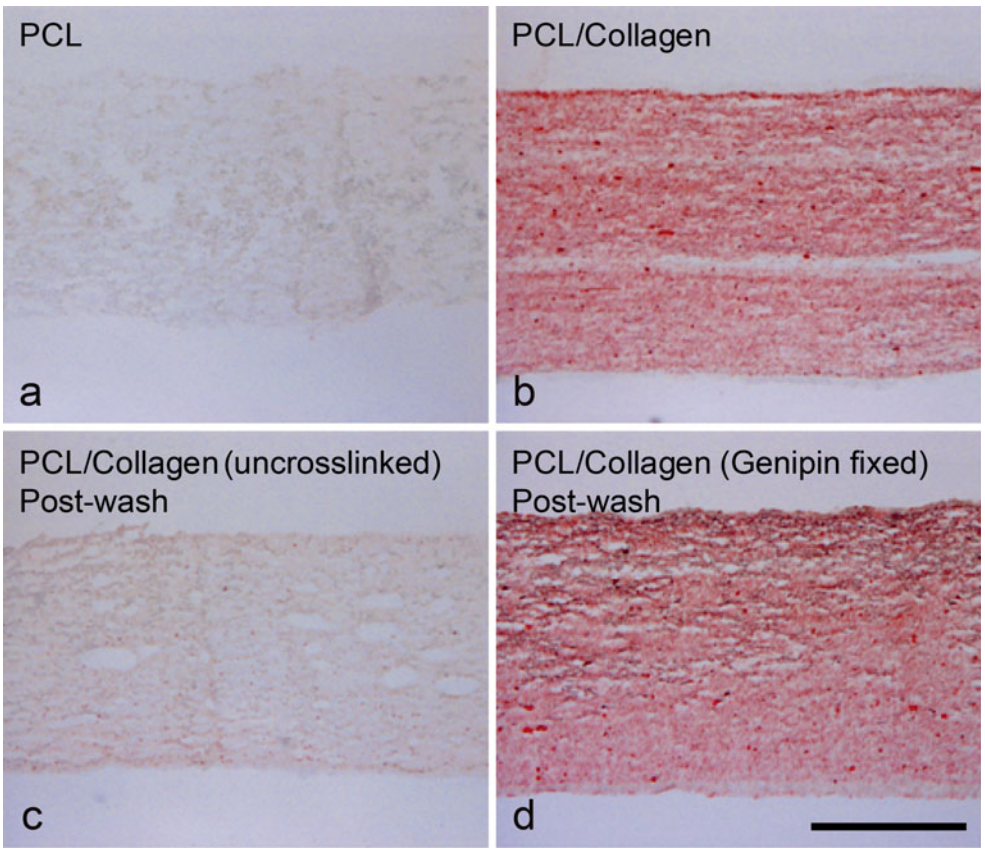

Fig. 4 Composite scaffolds containing biomimetic (collagen) and synthetic (PCL) fiber fractions. Picrosirius Red (*PSR*) staining of PCL (**a**) and composite (*Low*, **b**) constructs upon formation (*top row*, **a**, **b**) and composites after washes with (**d**) and without (**c**) GP crosslinking (*bottom row*, **c**, **d**). *Red staining* indicates presence and retention of collagen fiber fraction. *Bar* 500 μm

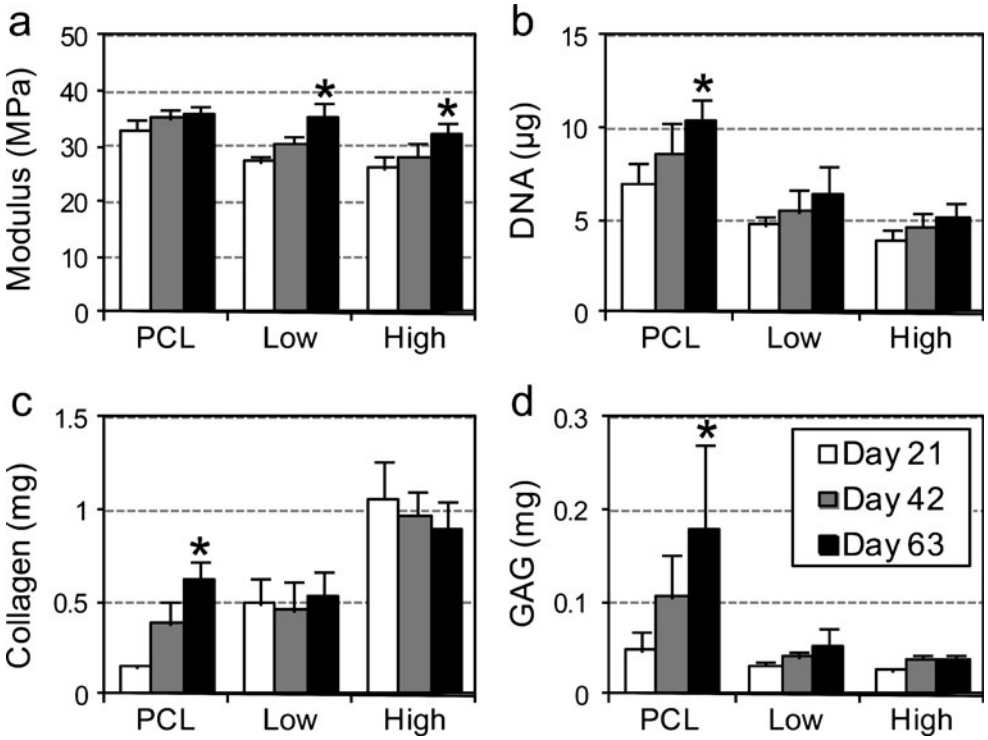

Fig. 5 Maturation of PCL and composite (Low and High) MSC-seeded collagen constructs over 9 weeks in culture. Modulus (**a**), DNA (**b**), collagen (**c**) and GAG (**d**) content of PCL and Low and High collagen composites as a function of culture duration. **P*<0.05 vs. day 21, *n*=6 per group

total cell number resided in this region in PCL controls. Conversely, in the innermost portion of the scaffold (i.e., 75%-100% infiltration), High and Low collagen composites contained only 3%-4% of the total cells in this region, whereas ~12% of total cells were present in this region in PCL constructs (*P*<0.05 vs. Low and High groups).

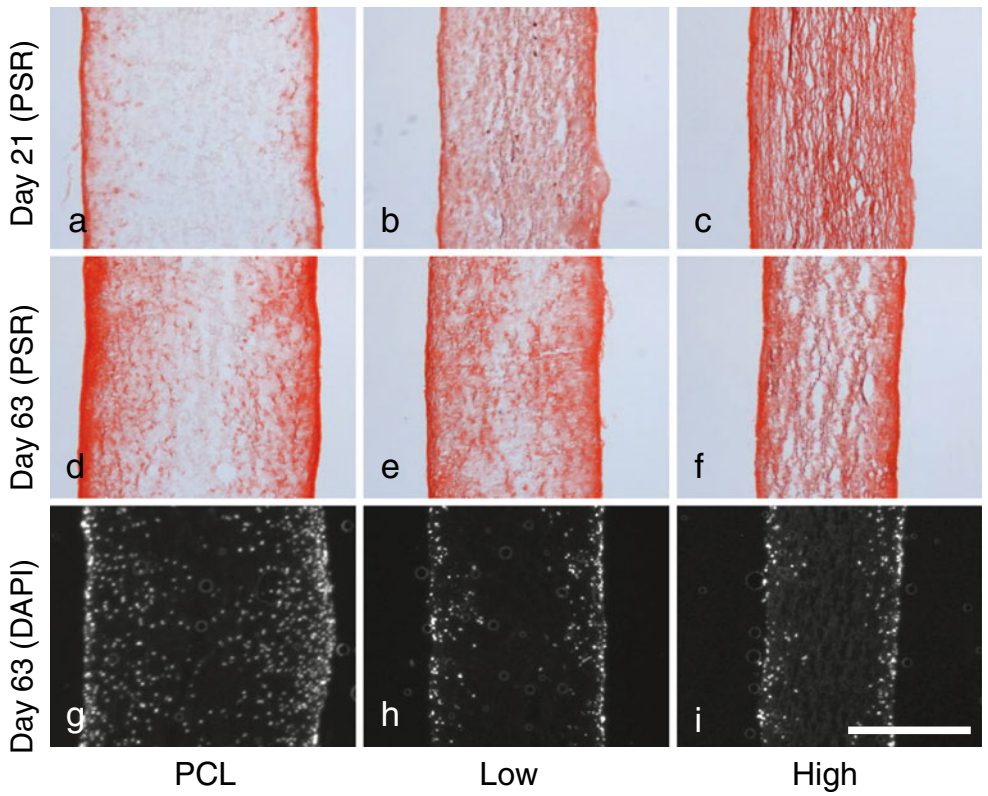

Fig. 6 Matrix deposition and cell infiltration in PCL (**a**, **d**, **g**) and composite (Low: **b**, **e**, **h**; High: **c**, **f**, **i**) MSC-seeded collage constructs at 9 weeks in culture. *Top two rows* Picrosirius Red (*PSR*) staining of cross sections from PCL and Low and High collagen composites on days 21 (**a–c**) and 63 (**d–f**), respectively. *Bottom row* (**g–i**) DAPI staining of cell nuclei (*punctate white staining* at scaffold border and in interior) of constructs on day 63. *Bar* 500 μm

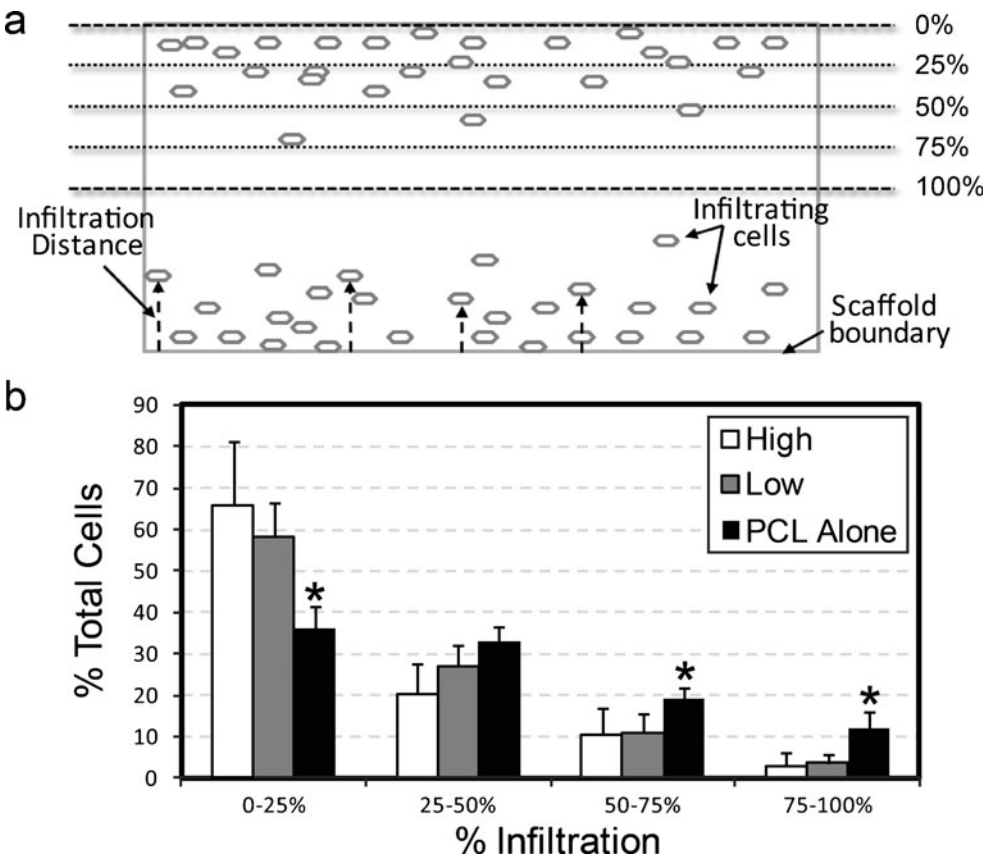

Fig. 7 Quantification of cell infiltration as a function of scaffold composition on day 63. **a** Representation of image processing algorithm highlighting the construct border, individual cell nuclei and their infiltration distance with respect to the boundary. The distance of each nuclei from the scaffold border was measured and binned into four regions, with 100% infiltration representing the centermost point of the scaffold cross section. **b** Percentage of total cells (at least 200 per image) in each quartile on day 63 as a function of composite formulation; High (high collagen content), Low (low collagen content) and PCL alone groups are shown. *$P<0.05$ compared with both High and Low groups within a given quartile, $n=5–6$ per group

Discussion

Although nanofibrous constructs are promising tools for soft tissue repair, the continued optimization of material elements, construction methods and culture systems is required to generate scaffolds that can promote functional repair in vivo. In particular, material composition that mimics the content of the native tissue might provide a biomimetic starting point for tissue development. As dense connective tissues such as the meniscus and the annulus fibrosus are composed of highly aligned collagen, we have produced aligned type I collagen nanofibrous scaffolds to mimic the natural composition and organization of these tissues. Consistent with nanofibrous scaffolds produced by using other polymer systems, fiber alignment imparts anisotropy as observed by the 8- to 10-fold higher modulus in the fiber direction compared with the direction perpendicular to fibers (Li et al. 2007). In the dry state, these aligned scaffolds match or exceed the mechanical properties of native tissue (i.e., on the order of 80 MPa; Bursac et al. 2009a, b; Skaggs et al. 1994). However, these as-formed constructs lack the complex packing and crosslinking that stabilizes native tissue structures (Bank et al. 1998; Powell and Boyce 2006; Verzijl et al. 2002; Birk et al. 1989, 1995; Birk and Zycband 1994) and so dissolve completely upon hydration, making them unsuitable for direct application.

To address this issue, a number of crosslinking methods have been developed to stabilize the nanofibrous form of collagen scaffolds. We have evaluated the potential of GP, a naturally occurring plant extract, to crosslink and stabilize collagen nanofibers. GP has been used in a number of studies to crosslink native tissue structures (i.e., valve leaflets) and engineered collagen-based materials (Sung et al. 2000, 2001; Liang et al. 2003, 2004; Solorio et al. 2010; Somers et al. 2008). In this study, GP-crosslinked fibers resist dissolution in aqueous solutions and maintain their fiber architecture; they do so to a greater extent than more traditional GA fixation methods. This is a promising finding, as GP is less cytotoxic than GA and is straightforward in its application. However, consistent with other crosslinking agents, the mechanical properties of GP-crosslinked scaffolds are similar to those of GA-fixed scaffolds after hydration, with both being markedly lower (80 times) than the as-spun dry scaffold (Barnes et al. 2007b). Collagen nanofibers fixed with either agent do however show more rapid and extensive MSC adhesion compared with PCL nanofibers. This enhanced adhesion, attributable to the biomimetic nature of collagen, might be important for enhancing cell invasion into thicker scaffolds but the low mechanical properties still limit applications to scenarios in which load-bearing is not a critical feature.

To address this persistent mechanical limitation, we next combined collagen and PCL together into a biomimetic and

biosynthetic composite scaffold. Here, the requisite mechanical properties are derived from the stiff synthetic component, whereas the collagen fiber fractions provide biomimetic instruction to promote cell adhesion and offer the potential for remodeling. By using a recently developed multi-jet spinning apparatus (Baker et al. 2009c), composite biomimetic/biosynthetic nanofibrous scaffolds can be formed. Staining for collagen in acellular scaffolds shows inclusion and retention of the collagen nanofibers within the composite (after GP crosslinking). These acellular scaffolds retain significant mechanical properties (on the order of 30 MPa) in the hydrated state, even at high (20%) levels of collagen fiber inclusion. Furthermore, direct measurements and histological staining reveal the persistence of graded levels of collagen content during culture. However, contrary to our initial hypothesis, the presence of the collagen fiber fraction at these levels does not improve matrix content, cell number, or infiltration. Indeed, the reverse has been observed, with the poorest infiltration and matrix deposition observed in composites containing the highest collagen fiber fraction (~20%). Of further note, little additional collagen and almost no proteoglycan are deposited in constructs containing collagen, whereas pure synthetic (PCL) constructs show an increase in both of these ECM components with time in culture.

Although the mechanism underlying these findings remains to be determined, the increased propensity for cells to adhere to collagen fibers might limit their fibrochondrogenic differentiation (production of proteoglycan and collagen) and division rates. In a recent study, we have shown that human MSCs are limited in their ability to differentiate on aligned PCL scaffolds compared with pellet culture (Baker et al. 2010). The collagen fibers may exacerbate this issue with bovine MSCs. Likewise, the DNA content in scaffolds containing collagen fiber fractions is ~two-fold lower; with fewer cells, less matrix will be formed in a given region. Further, high levels of collagen in the cellular microenvironment might down-regulate new collagen production in a negative feedback mechanism, as has been observed in other cell types (Buschmann et al. 1992). The enhanced adhesion with collagen fiber fraction inclusion might likewise have limited cell infiltration; more adherent cells might migrate to a lower extent than those with only moderate adhesion to synthetic fibers. Alternatively, GP crosslinking might have been too robust and so limited the ability of cells to remodel the matrix sufficiently to enable migration. Subcutaneous implantation of decellularized native tissues shows a dose-dependent decrease in cell colonization with extended GP treatment (Liang et al. 2004). Thus, an overly slow degradation of collagen fibers, coupled with a slight swelling of this fiber fraction with hydration, serves to limit pore size further in these composites. An additional concern might be the state of the collagen itself, with recent reports suggesting that HFIP (and electrospinning) denatures type 1 collagen, with the consequent loss of biologic epitopes (Zeugolis et al. 2008). Finally, the collagen fiber fraction might have simply been too low, such that negative effects prevailed over positive attributes. Despite our efforts to increase collagen fiber fractions by spinning from two jets (with only one PCL jet), the maximum collagen fiber fraction is only 20%. In our past work with sacrificial PEO fibers, a minimum threshold of 40% is required to improve cell infiltration relative to pure PCL scaffolds (Baker et al. 2008). As rapid cell colonization is essential for the clinical application of nanofibrous scaffolds for regenerative applications, future studies should elucidate the mechanism by which this limitation occurs in order to optimize biomimetic/synthetic composites for rapid construct maturation and to determine whether the temporal characteristics of this process change with in vivo implantation. Additionally, bioactive factors could be included in the collagen component to expedite infiltration of these meshes; in a recent study, by Ekaputra and colleagues, vascular endothelial growth factor and platelet-derived growth factor increased vascular cell invasion of PCL/collagen fibrous scaffolds containing hyaluronic acid based hydrogel inclusions (Ekaputra et al. 2011).

In conclusion, we generated aligned type I collagen fibrous scaffolds and composite biomimetic/synthetic hybrid constructs designed for the repair or replacement of dense connective tissues. GP crosslinking stabilizes collagen nanofiber morphology in both single-fiber and composite scaffold formulations, enabling the production of a mechanically robust nanofibrous network with biomimetic inclusions. Whereas these collagen fibers enhance initial cell adhesion, current findings do not support the use of collagen fiber fractions to improve cell infiltration, as the majority of cells in collagen-containing composites remain at the outer regions of the scaffold. Continuing studies will seek to optimize these findings by further increasing the collagen fraction while, at the same time, decreasing the degree of crosslinking in this fiber fraction, so as to make this portion of the composite more amenable to remodeling and eventual colonization. Alternatively, the same fiber fractions could be employed but fibers could be positioned via melt electrospinning to define fiber and pore structure specifically in the forming composite (Hutmacher et al. 2011; Dalton et al. 2006, 2009). Additionally, the inclusion of a separate rapid-pore-forming fiber fraction (i.e., sacrificial PEO fibers) into these dynamic biomimetic structures might improve this infiltration process. Ultimately, our work might provide a structurally and mechanically relevant framework of biosynthetic and biomimetic fibrous composites for in vivo tissue engineering.

References

Ayres C, Bowlin GL, Henderson SC, Taylor L, Shultz J, Alexander J, Telemeco TA, Simpson DG (2006) Modulation of anisotropy in electrospun tissue-engineering scaffolds: analysis of fiber alignment by the fast Fourier transform. Biomaterials 27:5524–5534

Baker BM, Mauck RL (2007) The effect of nanofiber alignment on the maturation of engineered meniscus constructs. Biomaterials 28:1967–1977

Baker BM, Gee AO, Metter RB, Nathan AS, Marklein RA, Burdick JA, Mauck RL (2008) The potential to improve cell infiltration in composite fiber-aligned electrospun scaffolds by the selective removal of sacrificial fibers. Biomaterials 29:2348–2358

Baker BM, Handorf AM, Ionescu LC, Li WJ, Mauck RL (2009a) New directions in nanofibrous scaffolds for soft tissue engineering and regeneration. Expert Rev Med Devices 6:515–532

Baker BM, Nathan AS, Huffman GR, Mauck RL (2009b) Tissue engineering with meniscus cells derived from surgical debris. Osteoarthritis Cartilage 17:336–345

Baker BM, Nerurkar NL, Burdick JA, Elliott DM, Mauck RL (2009c) Fabrication and modeling of dynamic multipolymer nanofibrous scaffolds. J Biomech Eng 131:101012

Baker BM, Nathan AS, Gee AO, Mauck RL (2010) The influence of an aligned nanofibrous topography on human mesenchymal stem cell fibrochondrogenesis. Biomaterials 31:6190–6200

Bank RA, Bayliss MT, Lafeber FP, Maroudas A, Tekoppele JM (1998) Ageing and zonal variation in post-translational modification of collagen in normal human articular cartilage. The age-related increase in non-enzymatic glycation affects biomechanical properties of cartilage. Biochem J 330:345–351

Barnes CP, Sell SA, Boland ED, Simpson DG, Bowlin GL (2007a) Nanofiber technology: designing the next generation of tissue engineering scaffolds. Adv Drug Deliv Rev 59:1413–1433

Barnes CP, Pemble CW, Brand DD, Simpson DG, Bowlin GL (2007b) Cross-linking electrospun type II collagen tissue engineering scaffolds with carbodiimide in ethanol. Tissue Eng 13:1593–1605

Birk DE, Zycband E (1994) Assembly of the tendon extracellular matrix during development. J Anat 184:457–463

Birk DE, Zycband EI, Winkelmann DA, Trelstad RL (1989) Collagen fibrillogenesis in situ: fibril segments are intermediates in matrix assembly. Proc Natl Acad Sci USA 86:4549–4553

Birk DE, Nurminskaya MV, Zycband EI (1995) Collagen fibrillogenesis in situ: fibril segments undergo post-depositional modifications resulting in linear and lateral growth during matrix development. Dev Dyn 202:229–243

Bursac P, Arnoczky S, York A (2009a) Dynamic compressive behavior of human meniscus correlates with its extra-cellular matrix composition. Biorheology 46:227–237

Bursac P, York A, Kuznia P, Brown LM, Arnoczky SP (2009b) Influence of donor age on the biomechanical and biochemical properties of human meniscal allografts. Am J Sports Med 37:884–889

Buschmann MD, Gluzband YA, Grodzinsky AJ, Kimura JH, Hunziker EB (1992) Chondrocytes in agarose culture synthesize a mechanically functional extracellular matrix. J Orthop Res 10:745–758

Buttafoco L, Kolkman NG, Engbers-Buijtenhuijs P, Poot AA, Dijkstra PJ, Vermes I, Feijen J (2006) Electrospinning of collagen and elastin for tissue engineering applications. Biomaterials 27:724–734

Casper CL, Yamaguchi N, Kiick KL, Rabolt JF (2005) Functionalizing electrospun fibers with biologically relevant macromolecules. Biomacromolecules 6:1998–2007

Casper CL, Yang W, Farach-Carson MC, Rabolt JF (2007) Coating electrospun collagen and gelatin fibers with perlecan domain I for increased growth factor binding. Biomacromolecules 8:1116–1123

Courtney T, Sacks MS, Stankus J, Guan J, Wagner WR (2006) Design and analysis of tissue engineering scaffolds that mimic soft tissue mechanical anisotropy. Biomaterials 27:3631–3638

Dalton PD, Lleixa Calvet J, Mourran A, Klee D, Moller M (2006) Melt electrospinning of poly-(ethylene glycol-block-epsilon-caprolactone). Biotechnol J 1:998–1006

Dalton PD, Woodfield T, Hutmacher DW (2009) Snapshot: polymer scaffolds for tissue engineering. Biomaterials 30:701–702

Ding B, Kimura E, Sato T, Fujita S, Shiratori S (2004) Fabrication of blend biodegradable nanofibrous nonwoven mats via multi-jet electrospinning. Polymer 45:1895–1902

Ekaputra AK, Prestwich GD, Cool SM, Hutmacher DW (2008) Combining electrospun scaffolds with electrosprayed hydrogels leads to three-dimensional cellularization of hybrid constructs. Biomacromolecules 9:2097–2103

Ekaputra AK, Prestwich GD, Cool SM, Hutmacher DW (2011) The three-dimensional vascularization of growth factor-releasing hybrid scaffold of poly (varepsilon-caprolactone)/collagen fibers and hyaluronic acid hydrogel. Biomaterials 32:8108-8117

Farndale RW, Buttle DJ, Barrett AJ (1986) Improved quantitation and discrimination of sulphated glycosaminoglycans by use of dimethylmethylene blue. Biochim Biophys Acta 883:173–177

Huang AH, Stein A, Tuan RS, Mauck RL (2009) Transient exposure to transforming growth factor beta 3 improves the mechanical properties of mesenchymal stem cell-laden cartilage constructs in a density-dependent manner. Tissue Eng Part A 15:3461–3472

Hutmacher DW, Dalton PD (2011) Melt electrospinning. Chem Asian J 6:44–56

Ionescu LC, Lee GC, Sennett BJ, Burdick JA, Mauck RL (2010) An anisotropic nanofiber/microsphere composite with controlled release of biomolecules for fibrous tissue engineering. Biomaterials 31:4113–4120

Kidoaki S, Kwon IK, Matsuda T (2005) Mesoscopic spatial designs of nano- and microfiber meshes for tissue-engineering matrix and scaffold based on newly devised multilayering and mixing electrospinning techniques. Biomaterials 26:37–46

Ladd MR, Lee SJ, Stitzel JD, Atala A, Yoo JJ (2011) Co-electrospun dual scaffolding system with potential for muscle-tendon junction tissue engineering. Biomaterials 32:1549–1559

Lee SJ, Yoo JJ, Lim GJ, Atala A, Stitzel J (2007) In vitro evaluation of electrospun nanofiber scaffolds for vascular graft application. J Biomed Mater Res A 83:999–1008

Li M, Mondrinos MJ, Gandhi MR, Ko FK, Weiss AS, Lelkes PI (2005a) Electrospun protein fibers as matrices for tissue engineering. Biomaterials 26:5999–6008

Li WJ, Mauck RL, Tuan RS (2005b) Electrospun nanofibrous scaffolds: production, characterization, and applications for tissue engineering and drug delivery. J Biomed Nanotechnol 1:259–275

Li WJ, Mauck RL, Cooper JA, Yuan X, Tuan RS (2007) Engineering controllable anisotropy in electrospun biodegradable nanofibrous scaffolds for musculoskeletal tissue engineering. J Biomech 40:1686–1693

Liang HC, Chang WH, Lin KJ, Sung HW (2003) Genipin-crosslinked gelatin microspheres as a drug carrier for intramuscular administration: in vitro and in vivo studies. J Biomed Mater Res A 65:271–282

Liang HC, Chang Y, Hsu CK, Lee MH, Sung HW (2004) Effects of crosslinking degree of an acellular biological tissue on its tissue regeneration pattern. Biomaterials 25:3541–3552

Ma Z, He W, Yong T, Ramakrishna S (2005) Grafting of gelatin on electrospun poly(caprolactone) nanofibers to improve endothelial cell spreading and proliferation and to control cell Orientation. Tissue Eng 11:1149–1158

Matthews JA, Wnek GE, Simpson DG, Bowlin GL (2002) Electrospinning of collagen nanofibers. Biomacromolecules 3:232–238

Mauck RL, Yuan X, Tuan RS (2006) Chondrogenic differentiation and functional maturation of bovine mesenchymal stem cells in long-term agarose culture. Osteoarthritis Cartilage 14:179–189

Mauck RL, Baker BM, Nerurkar NL, Burdick JA, Li WJ, Tuan RS, Elliott DM (2009) Engineering on the straight and narrow: the mechanics of nanofibrous assemblies for fiber-reinforced tissue regeneration. Tissue Eng Part B Rev 15:171–193

Nathan AS, Baker BM, Nerurkar NL, Mauck RL (2010) Mechano-topographic modulation of stem cell nuclear shape on nanofibrous scaffolds. Acta Biomater 7:57–66

Nerurkar NL, Elliott DM, Mauck RL (2007) Mechanics of oriented electrospun nanofibrous scaffolds for annulus fibrosus tissue engineering. J Orthop Res 25:1018–1028

Nerurkar NL, Baker BM, Sen S, Wible EE, Elliott DM, Mauck RL (2009) Nanofibrous biologic laminates replicate the form and function of the annulus fibrosus. Nat Mater 8:986–992

Pham QP, Sharma U, Mikos AG (2006a) Electrospinning of polymeric nanofibers for tissue engineering applications: a review. Tissue Eng 12:1197–1211

Pham QP, Sharma U, Mikos AG (2006b) Electrospun poly(epsilon-caprolactone) microfiber and multilayer nanofiber/microfiber scaffolds: characterization of scaffolds and measurement of cellular infiltration. Biomacromolecules 7:2796–2805

Powell HM, Boyce ST (2006) EDC cross-linking improves skin substitute strength and stability. Biomaterials 27:5821–5827

Rho KS, Jeong L, Lee G, Seo BM, Park YJ, Hong SD, Roh S, Cho JJ, Park WH, Min BM (2006) Electrospinning of collagen nanofibers: effects on the behavior of normal human keratinocytes and early-stage wound healing. Biomaterials 27:1452–1461

Sefcik LS, Neal RA, Kaszuba SN, Parker AM, Katz AJ, Ogle RC, Botchwey EA (2008) Collagen nanofibres are a biomimetic substrate for the serum-free osteogenic differentiation of human adipose stem cells. J Tissue Eng Regen Med 2:210–220

Sell SA, McClure MJ, Barnes CP, Knapp DC, Walpoth BH, Simpson DG, Bowlin GL (2006) Electrospun polydioxanone-elastin blends: potential for bioresorbable vascular grafts. Biomed Mater 1:72–80

Shields KJ, Beckman MJ, Bowlin GL, Wayne JS (2004) Mechanical properties and cellular proliferation of electrospun collagen type II. Tissue Eng 10:1510–1517

Skaggs DL, Weidenbaum M, Iatridis JC, Ratcliffe A, Mow VC (1994) Regional variation in tensile properties and biochemical composition of the human lumbar anulus fibrosus. Spine 19:1310–1319

Solorio L, Zwolinski C, Lund AW, Farrell MJ, Stegemann JP (2010) Gelatin microspheres crosslinked with genipin for local delivery of growth factors. J Tissue Eng Regen Med 4:514–523

Somers P, De Somer F, Cornelissen M, Bouchez S, Gasthuys F, Narine K, Cox E, Van Nooten G (2008) Genipin blues: an alternative non-toxic crosslinker for heart valves? J Heart Valve Dis 17:682–688

Stankus JJ, Freytes DO, Badylak SF, Wagner WR (2008) Hybrid nanofibrous scaffolds from electrospinning of a synthetic biodegradable elastomer and urinary bladder matrix. J Biomater Sci Polym Ed 19:635–652

Stegemann H, Stalder K (1967) Determination of hydroxyproline. Clin Chim Acta 18:267–273

Stella JA, Liao J, Hong Y, David Merryman W, Wagner WR, Sacks MS (2008) Tissue-to-cellular level deformation coupling in cell micro-integrated elastomeric scaffolds. Biomaterials 29:3228–3236

Stitzel J, Liu J, Lee SJ, Komura M, Berry J, Soker S, Lim G, Van Dyke M, Czerw R, Yoo JJ, Atala A (2006) Controlled fabrication of a biological vascular substitute. Biomaterials 27:1088–1094

Sung HW, Chang Y, Liang IL, Chang WH, Chen YC (2000) Fixation of biological tissues with a naturally occurring crosslinking agent: fixation rate and effects of pH, temperature, and initial fixative concentration. J Biomed Mater Res 52:77–87

Sung HW, Liang IL, Chen CN, Huang RN, Liang HF (2001) Stability of a biological tissue fixed with a naturally occurring crosslinking agent (genipin). J Biomed Mater Res 55:538–546

Telemeco TA, Ayres C, Bowlin GL, Wnek GE, Boland ED, Cohen N, Baumgarten CM, Mathews J, Simpson DG (2005) Regulation of cellular infiltration into tissue engineering scaffolds composed of submicron diameter fibrils produced by electrospinning. Acta Biomater 1:377–385

Teo WE, Ramakrishna S (2006) A review on electrospinning design and nanofibre assemblies. Nanotechnology 17:R89–R106

Venugopal J, Ma LL, Yong T, Ramakrishna S (2005) In vitro study of smooth muscle cells on polycaprolactone and collagen nanofibrous matrices. Cell Biol Int 29:861–867

Verzijl N, DeGroot J, Ben ZC, Brau-Benjamin O, Maroudas A, Bank RA, Mizrahi J, Schalkwijk CG, Thorpe SR, Baynes JW, Bijlsma JW, Lafeber FP, TeKoppele JM (2002) Crosslinking by advanced glycation end products increases the stiffness of the collagen network in human articular cartilage: a possible mechanism through which age is a risk factor for osteoarthritis. Arthritis Rheum 46:114–123

Yannas IV, Tzeranis DS, Harley BA, So PT (2010) Biologically active collagen-based scaffolds: advances in processing and characterization. Philos Transact A Math Phys Eng Sci 368:2123–2139

Zeugolis DI, Khew ST, Yew ES, Ekaputra AK, Tong YW, Yung LY, Hutmacher DW, Sheppard C, Raghunath M (2008) Electrospinning of pure collagen nano-fibres—just an expensive way to make gelatin? Biomaterials 29:2293–2305

Zhong S, Teo WE, Zhu X, Beuerman RW, Ramakrishna S, Yung LY (2006) An aligned nanofibrous collagen scaffold by electrospinning and its effects on in vitro fibroblast culture. J Biomed Mater Res A 79:456–463